Elasticity of Lyotropic Chromonic Liquid Crystals Probed by Director Reorientation in a Magnetic Field

Shuang Zhou, Yu. A. Nastishin, M. M. Omelchenko, L. Tortora, V. G. Nazarenko, O. P. Boiko, T. Ostapenko, T. Hu, C. C. Almasan, S. N. Sprunt, J. T. Gleeson, and O. D. Lavrentovich

Phys. Rev. Lett. **109**, 037801 — Published 18 July 2012

DOI: 10.1103/PhysRevLett.109.037801

Elasticity of lyotropic chromonic liquid crystals probed by director reorientation in magnetic field

Shuang Zhou[1], Yu. A. Nastishin[1,2], M. M. Omelchenko[1], L. Tortora[1], V. G. Nazarenko[3], O. P. Boiko[3], T. Ostapenko[4], T. Hu[4], C.C. Almasan[4], S. N. Sprunt[4], J. T. Gleeson[4], and O. D. Lavrentovich[1*]

[1] *Liquid Crystal Institute and Chemical Physics Interdisciplinary Program, Kent State University, Kent, Ohio 44242*

[2] *Institute of Physical Optics, 23 Dragomanov str., Lviv, 79005, Ukraine*

[3] *Institute of Physics, prospect Nauky 46, Kiev-39, 03039, Ukraine*

[4] *Department of Physics, Kent State University, Kent, Ohio 44242*

Using a magnetic Frederiks transition technique, we measured the temperature and concentration dependences of splay K_1, twist K_2, and bend K_3 elastic constants for the lyotropic chromonic liquid crystal (LCLC) Sunset Yellow, formed through non-covalent reversible aggregation of organic molecules in water. K_1 and K_3 are comparable to each other and are an order of magnitude higher than K_2. At higher concentrations and lower temperatures, K_1 and the ratios K_1/K_3, K_1/K_2 increase, which is attributed to elongation of self-assembled LCLC aggregates, a feature not found in conventional thermotropic and lyotropic liquid crystals formed by covalently bound units of a fixed length.

PACS numbers:

Soft non-covalent attraction of organic molecules in solutions often results in elongated aggregates [1–4]. Examples include "living polymers", wormlike micelles of amphiphiles, stacks of disk-like dye and drug molecules [1, 2], nucleic acids [4] and proteins. In a broad range of concentrations and temperatures, the self-assembled polydisperse aggregates of relatively rigid flat organic molecules form nematic and columnar liquid crystal (LC) phases, generally classified as lyotropic chromonic LCs (LCLCs) [1, 2]. Since the aggregates are bound by weak van der Waals forces, their length varies strongly with concentration, temperature, ionic content, making the LCLCs very different from thermotropic LCs with molecules of covalently fixed shape and from lyotropic LCs formed by objects such as tobacco mosaic viruses [5] or polymers of fixed molecular weight [6]. An intriguing question is how this fundamental structural feature of LCLCs reflects on their elastic properties.

Despite the growing interest in LCLCs, very little is known about their elasticity. Theory and numerical simulations have reached the level at which one can describe phase diagrams of LCLCs [7–9], but not their elastic moduli. The main challenge is in accounting for length distribution and flexibility of aggregates. The average length of aggregates $\bar{L}$ in the nematic LCLC can be estimated [10], following the work of van der Schoot and Cates [11] on wormlike surfactant micelles, as a function of stacking energy E, volume fraction ϕ of the chromonic molecules, persistence length λ_p of the LCLC aggregates of diameter D, and absolute temperature T:

$$\bar{L} = L_0 \phi^{5/6} (\frac{\lambda_p}{D})^{1/3} \exp \frac{E + \kappa\phi}{2k_B T}, \qquad (1)$$

where $L_0 = 2\pi^{-2/3}\sqrt{a_z D}$ is a length characterizing the size of a monomer, a_z is the period of molecular stacking along the aggregate, κ is a constant describing the enhancement of aggregation by the excluded volume effects; in the second virial approximation, $\kappa \approx 4k_B T$ [11]. Experimental characterization of elastic parameters is also challenging as it requires two types of uniformly aligned samples, with the director $\hat{\mathbf{n}}$ (average orientation of aggregates) being in plane of the cell (planar alignment) and perpendicular to it (homeotropic alignment). The elastic properties can then be determined by applying a magnetic field $\mathbf{B}$ to realign $\hat{\mathbf{n}}$ (Frederiks effect). Only planar cells were used so far. In these cells, $\mathbf{B}$ causes twist or mixed twist-bend of $\hat{\mathbf{n}}$, depending on the rate of field increase [12, 13]. Golovanov et al. [14, 15] used this effect to extract the twist constant $K_2 = 0.36$pN and the bend-twist ratio $K_3/K_2 = 12.2$ for disulphoindantrone-water LCLC.

In this letter, we take advantage of the new techniques to align the same LCLC in both planar and homeotropic fashion, and determine all three bulk elastic constants, in geometries where the field-induced director gradients are small and correspond to equilibrium states. We study aqueous solutions of disodium salt of 6-hydroxy-5-[(4-sulfophenyl)azo]-2-naphthalenesulfonic acid, also known as Sunset Yellow (SSY). In this LCLC, the disk-like molecules reversibly aggregate face-to-face and form elongated stacks with one molecule per cross section [16–18]. We find that dependences of K_1, K_2, K_3 on concentration c and temperature (t, in $^\circ C$) are highly unusual as compared to other classes of LCs and explain the results by the varying contour length and persistence length of self-assembled flexible polydisperse aggregates.

Samples and experimental set-up. SSY was purchased from Sigma Aldrich and purified as described in Ref. [16]. The study is performed for the nematic phase at c= 29.0, 30.0, and 31.5 wt % (ϕ=0.18, 0.19 and 0.20, respectively [10]) . The diamagnetic susceptibility mea-

sured parallel to $\hat{\mathbf{n}}$ is smaller than its orthogonal counterpart, $\Delta\chi = \chi_{\parallel} - \chi_{\perp} < 0$. We used a magnetometer with a superconducting quantum interference device and determined $\Delta\chi$ following Ref.[19] as $\Delta\chi = 3(\chi_{av} - \chi_{\perp})$, where $\chi_{av} = \frac{1}{3}(\chi_{\parallel} + 2\chi_{\perp})$ is the average volumetric magnetic susceptibility. The LC sample, flame-sealed in a glass tube and placed in the superconducting solenoid, was heated well above the nematic-to-isotropic transition and slowly cooled down to 25°C in presence of 5T field. $\chi_{av}(t)$ was measured in the isotropic phase and linearly extrapolated to the nematic phase region, following Ref [19]. At 25°C, the magnetization was monitored for over 10 hours until its value saturated, indicating an equilibrium homogeneous nematic state with $\hat{\mathbf{n}} \perp \mathbf{B}$, which allowed to determine $\chi_{\perp}$. An independent measurement of $\Delta\chi$ at 1T shows little ($\sim 1\%$) difference from the 5T data, indicating that the field-induced order is negligible, which is consistent with the data on Cotton-Mouton constant [20]. Mass densities were measured with a densitometer DE 45 (Mettler Toledo). At 25 °C and c=29.0 %, we find $\Delta\chi = (-7.2 \pm 0.7) \times 10^{-7}$.

To determine the elastic parameters, we used flat glass cells of thickness d=20-25 μm. A relatively large d and smallness of director gradients in the Frederiks effect help to avoid possible changes of scalar order parameter in a strongly distorted LCLC [21]. For planar alignment, the substrates were rubbed with a superfine abrasive paper (001K Crystal Bay^{TM} Crocus Cloth, 3M), washed, dried, and treated with UV ozone for 5 min to improve wettability. Homeotropic alignment of SSY was achieved with unrubbed polyimide SE-7511L (Nissan).

The cell is placed in the magnetic field and probed with two orthogonal polarized laser beams. One beam is parallel to $\mathbf{B}$. The normal to the cell, $\hat{\mathbf{z}}$, makes an angle α with $\mathbf{B}$, $\hat{\mathbf{y}}$ is the axis of rotation, and the $\hat{\mathbf{x}}$ axis is parallel to $\hat{\mathbf{n}}$ in the planar cell, FIG.1. The angle α is controlled with a precision better than 0.1 °.

Homeotropic cells, bend constant K_3. K_3 is determined by setting $\alpha = 0$ and detecting the optical phase retardation for the laser beam 1, transmitted through the cell and two pairs of crossed circular polarizers (each comprised of a linear polarizer and a $\lambda/4$ plate). The light transmission increases at the threshold

$$B_3 = \frac{\pi}{d}\sqrt{\frac{\mu_0 K_3}{-\Delta\chi}}, \qquad (2)$$

at which $\hat{\mathbf{n}}$ starts to tilt from the z-axis (μ_0 is the magnetic permeability constant). The circular polarizers allowed us to detect the tilt regardless of its direction. To avoid the possible effect of umbilics [22], we used beams of expanded cross section (≈ 2 mm^2); moving the sample in the xy plane did not change the values of B_3.

In principle, Eq.(2) might need a correction, $d \to d+l$, where l is the so-called surface anchoring extrapolation length [23]. We verified the validity of Eq.(2) by measuring $B_3 = 3.5$ T in ultrathin cells ($d \approx 4$ μm), using a 31 T solenoid at the National High Magnetic Field Laboratory (Tallahassee, FL). The result leads to l=0.15 μm, much smaller than d in the measurements of K_3, which validates Eq. (2).

We extracted B_3 from the hysteresis-free field dependences of transmitted light intensity obtained for a very low rate of field increments, 0.002 T/min [10]. Repeating measurements at different points of the cell and on different cells, we established that the results were reproducible within 5%. The temperature and concentration dependences of $K_3/(-\Delta\chi)$ determined from the threshold field B_3 are plotted in FIG 2(a).

Planar cells, splay constant K_1. The splay Frederiks transition for $\Delta\chi < 0$ requires a planar cell placed at $\alpha = 90°$, i.e., $\mathbf{B} \parallel \hat{\mathbf{n}}_0$, FIG. 1. However, as K_2 is about an order of magnitude smaller than K_1, FIG. 2, twist will develop before splay. To impose splay, we aligned the cell at α=25°. As B increases from 0 to 0.33 T,

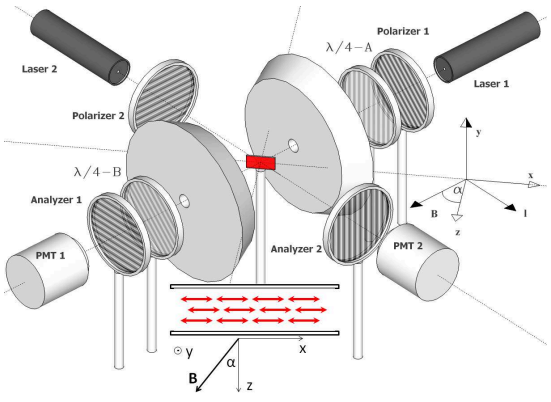

FIG. 1: (color online)Schematic of experiment setup. Sample is held in a hot stage for temperature control (not shown here). Both laser 1 and 2 are He-Ne lasers ($\lambda = 633$ nm).

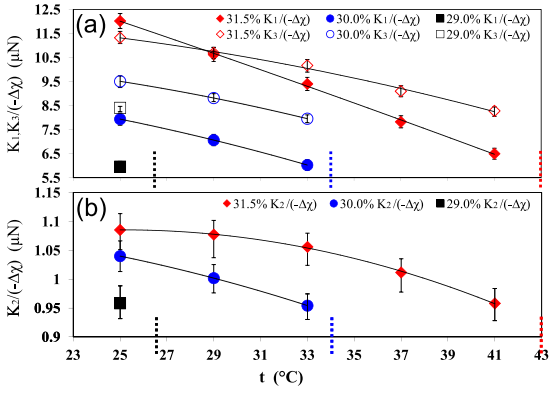

FIG. 2: (color online)Temperature and concentration dependences of (a) $K_{1,3}/(-\Delta\chi)$ and (b) $K_2/(-\Delta\chi)$. The vertical dash lines mark the nematic-biphasic transition temperature upon heating (same for other plots)

the director experiences threshold-less mixed splay-bend deformation. We measured the field dependence of optical retardation of the cell $R(B)$ by Senarmont technique [24]. The theoretical dependence $R(B)$ was determined by numerically calculating the profile of director tilt $\theta(z)$ (with resppect to the z-axis) from the bulk equilibrium equation [10]

$$\mathcal{F} = \frac{1}{2}(K_1 \sin^2\theta + K_3 \cos^2\theta)\theta'^2 - \frac{1}{2}\frac{\Delta\chi}{\mu_0}B^2\cos^2(\alpha-\theta). \quad (3)$$

Since $\frac{K_3}{-\Delta\chi}$ is already known, we fit the experimental $R(B)$ to extract $\frac{K_1}{-\Delta\chi}$ as the only fitting parameter, FIG 2(a).

Planar cells, twist constant K_2. The magnetic field applied parallel to $\hat{\mathbf{n}}$ in the geometry α=90° often leads to periodic distortions instead of the uniform twist [12–14]. To avoid this regime, we use α=75°. The increasing field first sets up a uniform splay, followed by a uniform twist above the threshold [10]:

$$B_2 \approx \frac{\pi}{d\sin\alpha}\sqrt{\frac{\mu_0 K_2}{-\Delta\chi}}. \quad (4)$$

We used the laser beam 2 polarized parallel to **B**, FIG 1. In the absence of twist, the propagating mode is purely extraordinary and is extinguished by the analyzer. When the field reaches B_2, the transmittance increases. Measuring B_2, we determine $\frac{K_2}{-\Delta\chi}$, FIG.2(b). The azimuthal anchoring length was small, $l_{az} \approx 0.15$ μm, as determined by measuring B_2 in thin cells with $d \approx 7$ μm. The optical response was hysteresis- free for the rate 0.002T/min of field change.

To determine the absolute values $K_{1,2,3}$ we used $\Delta\chi$ presented above for $t = 25$ °C, and found $K_1 = (4.3\pm0.4)$ pN, $K_2 = (0.7\pm0.07)$ pN, $K_3 = (6.1\pm0.6)$ pN for c=29.0 %. Comparing these to 5CB values [23], $K_1 = 6.6$ pN, $K_2 = 3$ pN, $K_3 = 10$ pN, one sees that K_1 and K_3 are of the same order but K_2 is much lower than that in 5CB. The SSY data are close to those for a lyotropic polymer LC (LPLC) formed by monodisperse poly-γ-benzyl glutamate (PBG) in organic solvents, with $\phi = 0.20$ and lenth-to-diameter ratio $L/D = 32$ [6]: $K_1 = 10$ pN, $K_2 = 0.6$ pN, $K_3 = 10$ pN.

The most dramatic and unusual (as compared to other types of LCs, either thermotropic or lyotropic, see, e.g., review by Singh [25]) trend observed in LCLC SSY is that the splay constant and its ratios such as $\frac{K_1}{K_3}$, $\frac{K_1}{K_2}$ increase when c increases and t decreases, Fig.3(b,c,d). As already indicated, the detailed theoretical interpretation tools to describe the elasticity of LCLCs are yet to come. We first compare the observed trends to the predictions of the phenomenological Landau-de Gennes (LdG) model [27] and models developed for LPLCs.

Within the LdG model, the temperature dependences of $K_{1,2,3}$, $\Delta\chi$, and Δn are determined by that of the scalar order parameter S, namely, $K_{1,2,3} \propto S^2$, $\Delta\chi, \Delta n \propto S$ [27]. We measured $\Delta n(t)$ and $S(t)$, using the technique described in [32], FIG.4. As seen from FIG. 3(a), only K_2 follows the LdG behavior, with $\frac{K_2}{-\Delta\chi S}$ being practically independent of t. In contrast, $\frac{K_1}{-\Delta\chi S}$, $\frac{K_1}{K_2}$, and $\frac{K_1}{K_3}$ decrease strongly when t increases, FIG. 3(b,c,d). Such a behavior is at odds not only with the LdG model, but also with the experiments for thermotropic LCs, which typically show $\frac{K_1}{K_3}$ and $\frac{K_1}{K_2}$ increasing with t [25].

In the models of LPLCs [28–31], the molecules of covalently fixed length $L = const$ and diameter $D \ll L$ are considered either as rigid or semiflexible. If the rods are rigid, the excluded volume theory [28] predicts $K_1 \propto \phi\frac{L}{D}$, $K_1/K_2 = 3$ and $K_3 \propto \phi^3(\frac{L}{D})^3$, so that $\frac{K_1}{K_3} \propto \phi^{-2}(\frac{D}{L})^2$, being much smaller than 1 and decreasing at high ϕ. The behavior of SSY is very different, with $K_1/K_2 \approx 6-11$ and $K_1 \approx K_3$; importantly, K_1/K_3 increases with $\phi \propto c$, Fig.3(d). The disagreement remains when one considers a bidisperse system [28] or takes into account electrostatic effects [30]. The SSY aggregates are charged, as the ionic groups at periphery dissociate in water. For the typical volume fractions of SSY in the nematic phase, $\phi \approx 0.2$, the Debye length λ_D is about 0.3 nm [18]. The electrostatic interactions lead to a "twisting effect", as two similarly charged aggregates tend to align perpendicularly to each other. The effect decreases K_2 by a small factor [30] $\approx (1-0.1h)$, where $h = \lambda_d/(D+2\lambda_d)$ is only about 0.2 for the nematic phase of SSY [18]. In LPLCs, the electrostatic effect might also increase K_3 [30] (thus making

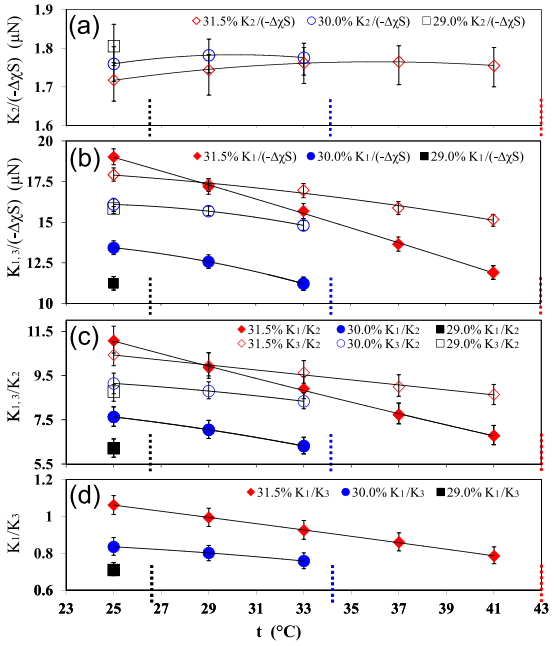

FIG. 3: (color online)Temperature and concentration dependences of (a) $\frac{K_2}{-\Delta\chi S}$, (b) $\frac{K_{1,3}}{-\Delta\chi S}$ and (c) $K_{1,3}/K_2$. (d)K_1/K_3

$\frac{K_1}{K_3}$ even smaller than in the model of non-charged rods), since the mutual repulsion of similar charges along the polymer makes it stiffer. We conclude that the elasticity of SSY cannot be described by the model of rigid rods of fixed length, whether charged or not, and turn to the models of semiflexible LPLCs [28–31].

The SSY aggregates should be flexible, as the attraction between monomers is weak, with the scission energy E in the range (7-11) k_BT [16, 18, 34]. In the theory of semiflexible LPLCs, K_2 and K_3 are determined by the persistence length λ_p of the polymers rather than by L [28, 29, 31]: $K_2 = \frac{k_BT}{D}\phi^{1/3}(\frac{\lambda_p}{D})^{1/3}$ [28]; $K_3 = \frac{4}{\pi}\frac{k_BT}{D}\phi\frac{\lambda_p}{D}$ (we use the standard definition [33] $\lambda_p = B/k_BT$ through the bend modulus B, which makes K_3 twice as large as in Ref. [31]). The last formula, with the experimental $K_3 = 6$pN at $\phi = 0.18$, $t = 25$ °C and $D = 1.1$nm [16, 18], yields $\lambda_p \approx 10$ nm. We are not aware of any other estimates of λ_p for LCLC, but the result appears reasonable when compared to $\lambda_p \approx 50$ nm for DNA duplex [33], as the latter is about twice wider than the SSY aggregate and we expect λ_p to increase with D.

The splay modulus K_1 still grows with the contour length L (as opposed to the persistence length λ_p) in flexible LPLCs: as explained by Meyer [3], splay deformations, under the condition of constant density, limit the freedom of molecular ends, which increases the entropy. Larger L implies a smaller number of molecular ends available to accommodate for splay and thus a higher K_1: $K_1 \approx \frac{4}{\pi}\frac{k_BT}{D}\phi\frac{L}{D}$ [31].

The model of semiflexible LCLC aggregates, supplemented by the idea that their *average* length $\bar{L}$ in LCLCs is not fixed [1–3, 11], Eq.(1), explains the observed T and ϕ dependences of elastic ratios, expressed as $\frac{K_1}{K_3} = \frac{\bar{L}}{\lambda_p}$, $\frac{K_1}{K_2} = \frac{4}{\pi}\phi^{2/3}\frac{\bar{L}}{\lambda_p^{1/3}D^{2/3}}$ and $\frac{K_3}{K_2} = \frac{4}{\pi}\phi^{2/3}(\frac{\lambda_p}{D})^{2/3}$. The dramatic decrease of $\bar{L}(\phi,t) \propto \exp(E/2k_BT)$ at elevated temperatures is expected to cause the strongest T-dependence of the splay constant K_1 . The persistent length is determined mainly by E and should be only a weak function of T and ϕ. Numerical simulations [8] show that $\lambda_p \propto 5 + 2.14E/k_BT$ for chromonic aggregates. Using this empirical result and Eq.(1), we thus estimate the trends as $\frac{K_1}{K_3} \propto \phi^{5/6}\frac{\exp((E+\kappa\phi)/2k_BT)}{(E/k_BT)^{2/3}}$, $\frac{K_1}{K_2} \propto \phi^{3/2}\exp((E+\kappa\phi)/2k_BT)$, and $\frac{K_3}{K_2} \propto \phi^{2/3}(E/k_BT)^{2/3}$. All three ratios increase when T decreases and ϕ increases, as in the experiment, FIG.3(c,d). The ratio K_1/K_2 is the most sensitive to ϕ and T, in a good agreement with FIG.3(c). The strong increase of $\frac{K_1}{K_2}$ with c explains the effect of spontaneous chiral symmetry breaking in osmotically condensed LCLC tactoids [26]. The estimate $K_1/K_3 = \bar{L}/\lambda_p$ combined with the experimental fact that $K_1/K_3 = 1.1 - 0.7$, FIG. 3(d), implies that $\bar{L}$ and λ_p are of the same order and that $\bar{L}/\lambda_p$ decreases at high temperatures, where the aggregates shorten while SSY approaches the isotropic phase. From the tilt of temperature dependencies, $\frac{K_3}{K_1}\frac{d(K_1/K_3)}{dT}$ and $\frac{K_2}{K_1}\frac{d(K_1/K_2)}{dT}$, we deduce $E \approx 10k_BT$ and $13k_BT$, respectively (for $\kappa = 4k_BT$ [11]).

To conclude, we measured the temperature and concentration dependences of Frank moduli of the self-assembled nematic LCLC. K_1 and K_3 are found to be comparable to each other and to the corresponding values in thermotropic LCs, while K_2 is one order of magnitude smaller. The splay constant K_1 and the elastic ratios $\frac{K_1}{K_3}$, $\frac{K_1}{K_2}$ increase significantly when the concentration of SSY increases or the temperature decreases. This unusual behavior is explained within a model of semiflexible SSY aggregates, the average length of which increases with concentration and decreases with temperature, a feature that is absent in conventional thermotropic and lyotropic LCs formed by units of fixed length.

This work was supported by NSF DMR grants 076290, 11212878, 1006606 and 0844115, by the Ministry of Education, Science, Youth and Sport of Ukraine (Grant No. 0111U010235), by Grants DFFD F35/534-2011 and NASU 1.4.1B/10, and by ICAM Branches Cost Sharing Fund from the Institute of Complex Adaptive Matter. Work performed at the National High Magnetic Field Laboratory is supported by NSF DMR-0084173, the State of Florida, and the US Department of Energy.

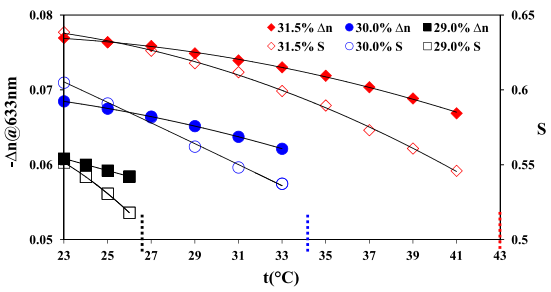

FIG. 4: (color online)Temperature and concentration dependences of Δn (at 633nm) and scalar order parameter S.

* Electronic address: olavrent@kent.edu

[1] J. Lydon, Liquid Crystals. **38**, 1663 (2011)
[2] A.J. Dickinson, N.D. LaRacuente, C.B. McKitterick, P. J. Collings, Mol. Cryst. Liq. Cryst. **509**, 9 (2009).
[3] R. B. Meyer, in *Polymer Liquid Crystals*, edited by A. Ciferri, W. R. Krigbaum, and R. B. Meyer (New York, Academic Press, 1982).
[4] M. Nakata, G. Zanchetta, B. D. Chapman, C. D. Jones, J. O. Cross, R. Pindak, T. Bellini, N. A. Clark, Science, **318**, 1276 (2007).
[5] Z. Dogic, S. Fraden, Curr. Opin. Colloid & Interf. Sci, **11**, 47 (2006).
[6] S.D. Lee, R.B. Meyer, Phys. Rev. Lett., **61**, 2217 (1988).
[7] F. Chami, M.R. Wilson, J. Am. Chem. Soc., **132**, 7794 (2010).

[8] T. Kuriabova, M.D. Betterton, M.A. Glaser, J. Mater. Chem. **20**, 10366 (2010).

[9] C. De Michele, T. Bellini, F. Sciortino, Macromolecules **45**, 1090 (2012).

[10] See Supplemental Material at [URL will be inserted by publisher] for the discussion of average aggregate length, diamagnetic anisotropy measurements, volume fraction, hysteresis of Frederiks effect, calculations of field-induced distortions and optical retardation.

[11] P. van der Schoot, M.E. Cates, Europhys. Lett. **25**, 515 (1994).

[12] F. Lonberg, S. Fraden, A. J. Hurd, and R. E. Meyer Phy. Rev. Lett. **52**, 1903 (1984).

[13] Y. W. Hui, M. R. Kuzma, M. San Miguel, and M. M. Labes, J. Chem. Phys. **83**, 288 (1985).

[14] A.V. Golovanov, A.V. Kaznacheev, A.S. Sonin, Izvestiya Akad. Nauk, Ser. Fiz. **59**, 82 (1995).

[15] A.V. Golovanov, A.V. Kaznacheev, A.S. Sonin, Izvestiya Akad. Nauk, Ser. Fiz. **60**, 43 (1996).

[16] V. R. Horowitz, L. A. Janowitz, A. L. Modic, P. A. Heiney, and P. J. Collings, Phys. Rev. **E72**, 041710 (2005).

[17] D. J. Edwards, J. W. Jones, O. Lozman, A. P. Ormerod, M. Sintyureva and G. J. T. Tiddy, J. Phys. Chem. **B 112**, 46, 14628 (2008).

[18] H.S. Park, S.W. Kang, L. Tortora, Yu. Nastishin, D. Finotello, S. Kumar, O.D. Lavrentovich, J. Phys. Chem. **B 112**, 16307 (2008)

[19] M. Stefanov, A. Saupe, Mol. Cryst. Liq. Cryst. **108**, 309 (1984).

[20] R.J. Luoma, Ph.D. Thesis, Brandeis University, 1995

[21] V. G.Nazarenko, O. P. Boiko, H.-S. Park, O. M. Brodyn, M. M. Omelchenko, L. Tortora, Yu.A. Nastishin, and O. D. Lavrentovich. Phys. Rev. Lett. **105**, 017801 (2010)

[22] M. Gu, I. I. Smalyukh, and O. D. Lavrentovich, Appl. Phys. Lett. **88**, 061110,(2006).

[23] M. Kleman and O.D. Lavrentovich, Soft Matter Physics: An Introduction (Springer-Verlag, New York, 2003).

[24] A. Nych, M. Voronin, V. Pergamenshchik, Yu, Kolomzarov, V. Sorokin and V. Nazarenko, Mol. Cryst. Liq. Cryst., **384**, 77 (2002)

[25] S. Singh, Physics Reports **277**, 283 (1996)

[26] L. Tortora and O. D. Lavrentovich, Proc. Natl. Acad. Sci. USA **108**, 5163 (2011)

[27] P. G. de Gennes and J. Prost, *The Physics of Liquid Crystals*, 2nd ed. (Oxford, Clarendon Press, 1993).

[28] T. Odijk, Liq. Cryst. 1, 553 (1986)

[29] A. Yu. Grosberg, A.V. Zhestkov, Polymer Sci. USSR **28**, 97 (1986)

[30] G.J. Vroege, T. Odijk, J. Chem. Phys. **87**, 4223 (1987)

[31] V.G. Taratuta, F. Lonberg, R.B. Meyer, Phys. Rev. A **37**, 1831 (1988)

[32] Yu. A. Nastishin, H. Liu, T. Schneider, V. Nazarenko, R. Vasyuta, S.V. Shiyanovskii and O.D. Lavrentovich, Phys. Rev. **E72**, 041711 (2005).

[33] A.A. Kornyshev, D.J. Lee, S. Leikin, A.Wynveen, Rev. Mod. Phys. **79**, 943 (2007)

[34] M.P. Renshaw and I.J. Day, J. Phys. Chem. **B 114**, 10032 (2010)